Appl. Phys. B 68, 801–805 (1999) / DOI 10.1007/s003409900038

Applied Physics B
Lasers
and Optics
© Springer-Verlag 1999

Photorefractive $LiNbO_3$ waveguides fabricated by combining He-implantation and copper exchange

S.M. Kostritskii[1], **P. Moretti**[2]

[1] Physics Dept, Kemerovo State University, Krasnaya str.6, Kemerovo, 650043 Russia
(Fax: +7-384/2525-383, E-mail: root@chsb.kemgu.kemerovo.su)
[2] Laboratoire de Physico-Chimie des Matériaux Luminescents, Université Claude Bernard Lyon I, 69622 Villeurbanne, France
(Fax: +33-78/897-410, E-mail: pmoretti@pcml.univ-lyon1.fr)

Received: 23 November 1998/Revised version: 15 February 1999/Published online: 12 April 1999

Abstract. We report on the fabrication and properties of He-implanted waveguides in lithium niobate, which are additionally doped with copper by using an ion-exchange process. We show that the photorefractive sensitivity in the waveguides is increased by a factor of 3000.

PACS: 78.20

Investigations are extensively increasing to search for new efficient methods of photorefractive waveguide fabrication for applications in integrated optics such as optical switching, resonant filtering, or holographic memory [1]. Most of the developmental efforts are centered on the use of lithium niobate ($LiNbO_3$) crystals, especially because of their ready commercial availability and well-established techniques for fabricating optical waveguides in this material, namely titanium diffusion [2], proton exchange [3], and ion implantation [4]. The photorefractive sensibility of the crystal can be strongly enhanced by incorporation in the latter suitable metal, ions, i.e. iron or copper, by using either the classical melt-doping procedure or surface doping methods, such as indiffusion or exchange. These are more sophisticated, but more promising. They are very accommodating since they can be directly combined with the related waveguide elaboration process [5, 6]. Besides, as a low-temperature process ($< 300\,^{\circ}C$), the new method of combined proton and copper exchange recently reported [6–8] is particularly attractive because it can also be applied to low-Curie-temperature compounds such as $LiTaO_3$ [9].

However, it has been shown that the electro-optic coefficients (EOC) are degraded in proton-exchange waveguides [8, 10], now it is well known that large EOC are of great advantage for holographic recording.

In contrast, no degradation of the EOC is observed in waveguides fabricated by light ion implantation [11], and furthermore, high-efficiency photorefractive waveguides have been recently obtained in SBN [12].

Dedicated to Prof. Dr. Eckard Krätzig on the occasion of his 60th birthday.

Therefore, our aim is to improve the photorefractive properties of copper-doped $LiNbO_3$ waveguides by using the following procedure: (i) to form single-mode optical waveguides by ion implantation, and (ii) to subsequently increase the photorefractive sensitivity of the crystal by performing a combined proton and copper exchange process in specific conditions, namely by minimizing the proton exchange. We thus expect in this case to avoid any significant degradation of the electro-optical effect in the crystal and, additionally, to induce weak changes only of the effective refractive index (insufficient to guide modes) by the exchange process itself.

We report for the first time on the fabrication and the study of the photorefractive properties of $LiNbO_3$ waveguides elaborated by helium implantation and subsequently doped by an ion-exchange process.

1 Waveguide formation

Alternatively to the exchange or diffusion methods, light-ion implantation (He^+ or H^+) can be applied to fabricate efficiently waveguides in crystals, including $LiNbO_3$ [12–16]. Note that the effect of the implantation is to generate an optical barrier whose thickness and position beneath the surface depend on the ion energy.

Optical-grade $LiNbO_3$ substrates (*Y* and *Z* cuts), typically of $5\,mm \times 10\,mm \times 1\,mm$ dimensions are used. Multiple implantation is performed (at room temperature) in order to enlarge the thickness of the optical barrier and to therefore obtain a better confinement of the light in the waveguides. Three helium implantations at slightly different energies and doses are thus successively performed to attempt to tailor approximately rectangular-like concentration profiles. The total implantation doses are either 1 or 2×10^{16} ions/cm^2. The energy values are 900, 1000, and 1100 keV, and 650, 725, and 800 keV for the sample series denoted A and B, respectively. As seen in Fig. 1, the resulting concentration profiles calculated by TRIM or Profile-Code simulation [17], which are indications of the shape of the optical barriers, extend in these cases from 2.1 to 2.8 μm and 1.4 to 2.0 μm, respectively. From previous investigations [11, 12, 15] of the effects of the

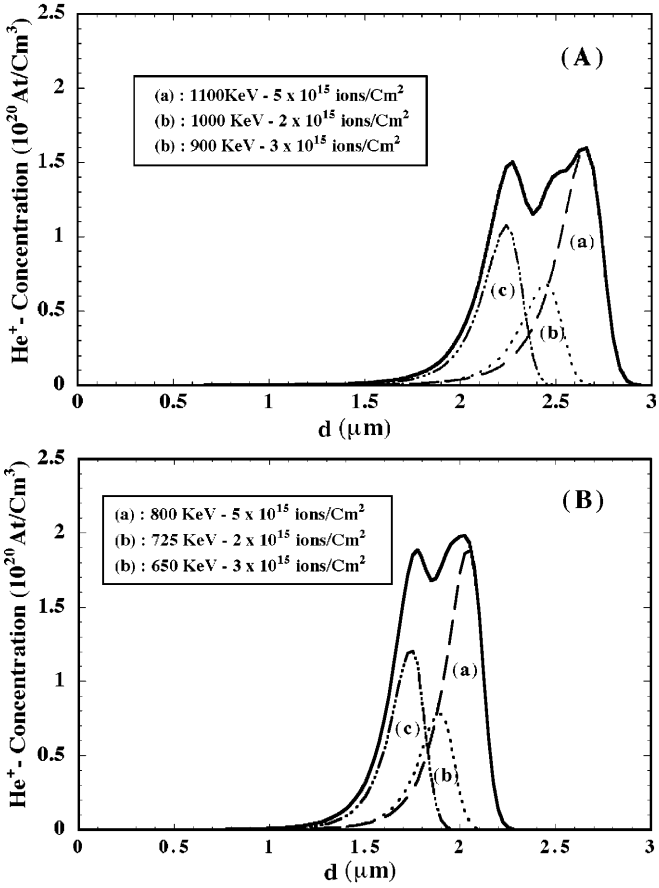

Fig. 1. He+ ion concentration profiles related to the two sample sets, **A** and **B** (see text and Table 1), calculated for multiple-like implantation in $LiNbO_3$ with a total dose of 1.0×10^{16} ions/cm^2 (Profile-code simulation program). The *dotted curves* are the summation of (a), (b), and (c)

implantation parameters (i.e. the energy and the dose of the ions) on the refractive-index variations in the implanted layer, we expect to create single-mode planar waveguides.

2 Exchange process

In previous works relevant to the fabrication of copper-doped photorefractive waveguides by exchange process the following procedure is used. A proton-exchanged layer is first formed in a melt of benzoic acid and then this layer is doped in another mixture of molten benzoic acid and copper oxide (or copper acetate) at generally different duration conditions [6–8].

In this study, after the preparation of the waveguides by ion implantation, a combined proton and copper exchange is performed in a single melt of benzoic acid mixed with lithium benzoate (LB) and copper acetate. The duration of the treatments ranges from 20 to 40 min at 230 °C. This low-temperature process is chosen as a first approach, in order to be sure not to destroy the optical barrier formed by ion implantation [18].

It is well known that the presence of LB in a molten benzoic acid acts as a buffer in the lithium–proton exchange process. We found here that for 3.2 mol. % lithium benzoate (LB) content, the proton exchange becomes insignificant in the presence of copper acetate with concentration above 1 mol. % in the melt. These concentration values of admixture can be considered as low-threshold limits, when some proton exchange can still be observed, not enough however to induce a meaningful change of the extraordinary refractive index. We found that a further increase of any of these two components in the melt leads to a sharp decrease of the proton exchange rate. No waveguiding layers can therefore be formed for such high-LB content, as confirmed by m-lines spectroscopy performed in non-implanted samples (see Sect. 4).

All the photorefractive waveguides investigated here have been obtained in these particular conditions, by treatment in molten benzoic acid mixed with LB and copper acetate at concentration levels varying from 3.0 to 3.6 mol. % and 0.8 to 4 mol. %, respectively.

3 Optical characterization

Optical absorption spectroscopy is performed in UV–visible and infrared ranges, by using differential methods with undoped samples as references. The copper and hydrogen contents in the samples are thus determined on the base of previous data obtained on combined proton- and copper-exchanged waveguides [6–8].

The values of the optical density measured at 26 315 cm^{-1} for the Cu^+ ion characteristic band (not given here) are very weak, from 0.01 to 0.05, which correspond to a copper concentration of the order of 0.012 mol. %–0.06 mol. %.

The intensity of the OH-vibration band for the various samples, measured by IR-absorption spectroscopy, is reported in Fig. 2a,b (see the samples notation in Table 1). The amplitude and the shape of this band (Fig. 2a), as compared to those of the unexchanged sample, clearly depend on the treatment conditions. In most samples the structure of the exchanged layer is almost entirely composed of the α phase of the $Li_{1-x}H_xNbO_3$ system, with low x values ranged approximately from 0.005 to 0.03. Accordingly, only very weak variation of the EOC ($\leq 3\%$) and of the refractive indices

Table 1. Results obtained for two series, A and B, (see text for the implantation energy) of He-implanted waveguides subsequently doped by a combined proton and copper exchange process. The total dose (multiple implantation is performed, see Fig. 1) is 1.0×10^{16} ions/cm^2 and 2.0×10^{16} ions/cm^2 for the A_3, A_4 samples, and the others, respectively. Reported are: the cut direction, the exchange parameters, the optical density δD_{Cu} of the copper-induced band at 380 nm, the saturated value of the light-induced refractive index change Δn^s (in 10^{-5}), and the estimated values of the photorefractive sensitivity S

Waveguide notation	Cut	Concentration of lithium benzoate /mol.%	Concentration of copper acetate /mol.%	Duration of ionic exchange /min	δD_{Cu}	Δn^s /10^{-5}	S/m^2 J^{-1}
A_1	*Y*	3.4	2.0	20	0.012	50	2.4×10^{-9}
A_2	*Z*	3.4	0.8	30	0.007	15	7.9×10^{-10}
A_3	*Y*	3.0	2.0	40	0.023	4.4	6.7×10^{-11}
A_4	*Z*	3.4	4.0	30	0.025	27	8.6×10^{-10}
B_1	*Z*	3.6	1.0	30	0.010	43	1.0×10^{-8}
B_2	*Z*	3.2	1.0	30	0.010	15	1.3×10^{-10}
B_3	*Y*	3.2	4.0	40	0.035	16	2.2×10^{-10}
B_4	*Y*	0	0	0	0.000	1.6	3.0×10^{-12}

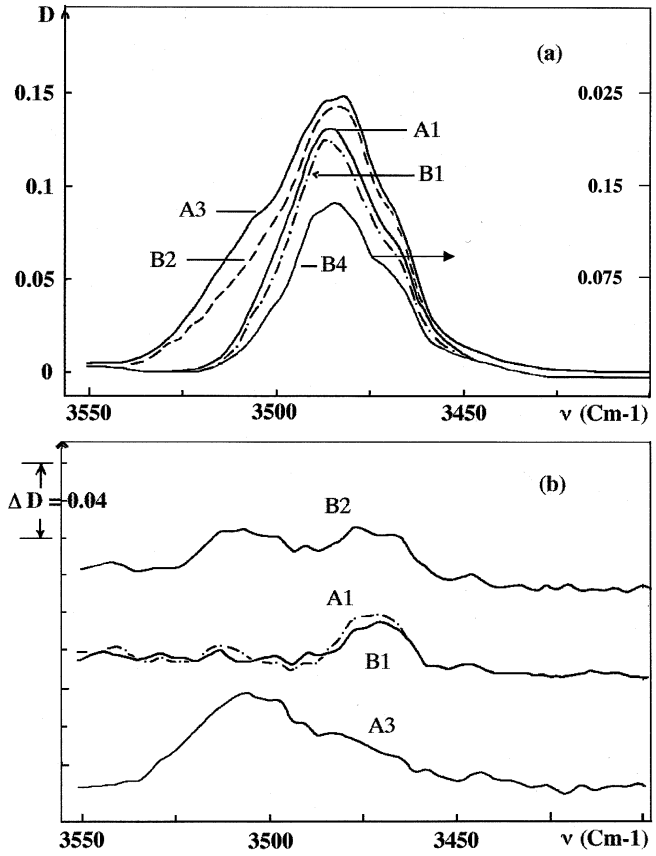

Fig. 2a,b. IR-absorption spectroscopy in the range of the OH-vibration band. The *curves* are labeled according to the samples notation used in Table 1. **a** Comparison of the spectra (optical density) of the various samples. Note that B4 is related to the undoped sample (as implanted). **b** Differential spectra obtained with the B4 sample as reference

($\leq 0.2\%$) are expected [7, 19], which is confirmed by the waveguides investigation (see below).

However, for the A_3 sample, whose related x value is 0.08, a weak shoulder emerges at 3508 cm^{-1} in the OH band. This component is better evidenced in the differential spectra given in Fig. 2b and allows us to assume the presence of a strongly protonated β_1 phase in the upper part of the exchanged layer [19]. Note that this component is also present, but to a lesser extent, in the B_2 sample ($x = 0.05$). Consequently we may expect [4] a significant degradation of the electro-optical effect in these samples, and even more in A_3.

Note that in this study we decide to limit the exchange temperature to 230 °C, in order to avoid a possible blurring of the He-implanted barrier layer [18]. We must emphasize that a copper-exchanged $LiNbO_3$ layer with small x values is not easy to obtain at this relatively low temperature. Efficient copper exchange has been only demonstrated up to now together with (or after) a consequent proton-exchange process and at higher temperature [7–9].

4 Waveguide characterization

The waveguiding properties are characterized by m-line spectroscopy at several excitation wavelengths, i.e. at 632.8 nm, 514.5, and 441.6 nm, with a He-Ne, argon, and He-Cd laser beam, respectively.

All photorefractive waveguides investigated here (see Table 1) have been obtained by treatment in a molten benzoic acid mixed with high content of LB and copper acetate. No waveguiding layers can be formed for such high-LB content, as we verify by performing m-lines spectroscopy at 632.8 nm in non-implanted samples.

The effective indices of the implanted waveguides are measured before and after the exchange process by dark-line spectroscopy. For extraordinarily polarization (i.e., TM and TE mode in the Z-cut and in the Y-cut samples, respectively) the waveguides are monomode for excitation wavelengths of 441.6 and 514.5 nm, confirmed by bright-line spectroscopy. The extraordinary index values found in the various samples at 632.8 nm are $n_e = 2.215$ for A_1, A_2, $n_e = 2.210$ for A_3, A_4 and $n_e = 2.213$ for all the B series. Note that one leaky mode is also observed in A_1 and A_2 ($n_e = 2.203$) samples, and that there is no fundamental difference regarding the waveguiding properties between the Y- and Z-cut samples.

In contrast, the waveguides are multimode (supporting two or three modes, including leaky modes) for ordinary polarization, but the ordinary index values are of no interest for our purpose, since the photorefractive response is 15 times smaller for that configuration and will not reported there.

Finally, we don't observe any significant changes of the effective refractive indices, for the extraordinarily polarized TM_0 and TE_0 modes, following the exchange process, in all our He-implanted waveguides. The index modifications are of the order, or less, of the measurement accuracy ($\Delta n = 5–8 \times 10^{-4}$). We can conclude therefore that the specific conditions we use for the formation of the exchanged layers are inconsequential on the waveguiding properties.

5 Photorefractive properties

The photorefractive properties of the planar waveguides are investigated by waveguide Raman spectroscopy. The high effectiveness of this method has been recently demonstrated [6].

The Raman intensity (I_R) is measured at $\lambda = 441.6$ nm, with an extraordinarily polarized light coupled in the waveguide, by using a 90° scheme [6] in the Stokes region, at a spectrum frequency shifted by 152 cm^{-1} from the frequency of the laser radiation. The monochromator slit is parallel to the top surface of the planar waveguide. The laser beam excites the Raman scattering simultaneously to the photoinduced light scattering, which is a direct consequence of the photorefractive effect.

In the absence of photorefractive activity, I_R is classically independent of excitation time. However, when a laser irradiation is launched into a photorefractive planar waveguide, I_R coming from a region limited by the optical system and entering into the monochromator slit decreases with time. This decrease is the consequence of the spreading of the pumping beam into a fan because of the time dependence of the photoinduced light scattering. As described in previous works [6], we assume that the time dependence of I_R coincides with the kinetics of the build up of the photorefractive effects and that the time constant τ of the exponential-like decay of I_R depends on the copper concentration in the waveguides. This exponential behavior is well observed in all our

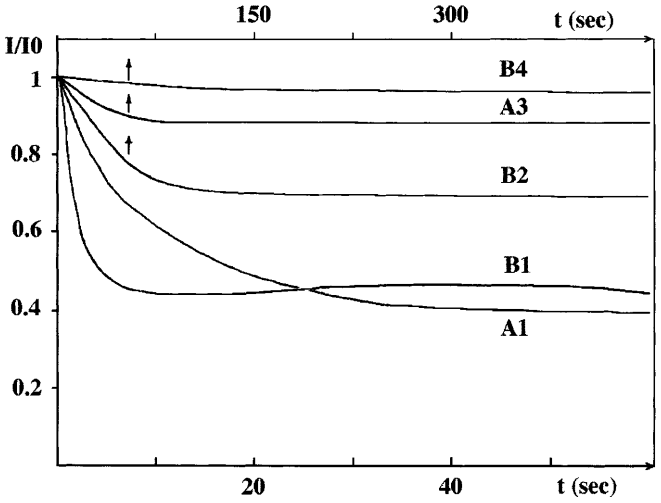

Fig. 3. Time evolution (related to the build up of the phorefractive effect) of the Raman intensity (I) measured at $\lambda = 441.6$ nm in a 90° scheme, for an injected power in the waveguides of $P_{in} = 0.3$ mW (The estimated power density is 12×10^4 W/m^2). The *curves* are labeled according to the sample notation used in Table 1

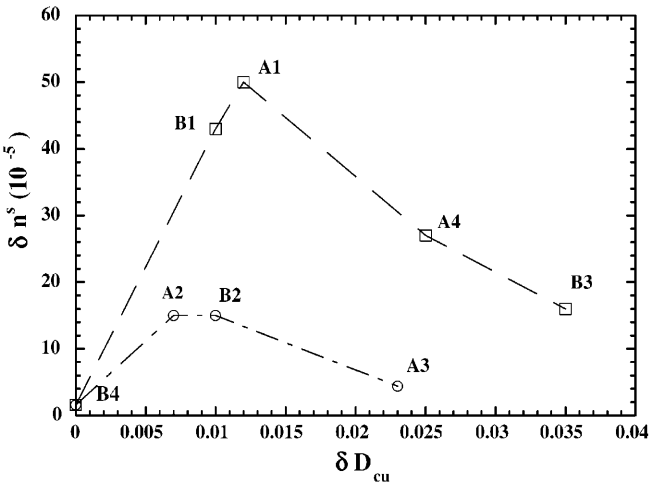

Fig. 4. Light-induced refractive index change (Δn^s) in saturation state (see Table 1 for the labelling of the dots) versus the copper-induced increment of the optical density (δD_{Cu}) measured by absorption spectroscopy; δD_{Cu} is proportional to the copper content in the samples. The *lines* are merely guides for the eye. These *lines* correspond to two different levels of hydrogen concentration, x_I (1) and x_{II} (2) with $x_I < x_{II}$ in the waveguiding layer after the combined proton and copper exchange

waveguides, as illustrated in Fig. 3, where it is clearly seen that the kinetics depends on the exchange conditions.

The relative change of the Raman signal amplitude, $\Delta I_R = I_{R0} - I_{RS}$, where I_{R0} is the Raman intensity at the initial stage (at $t = 0$), and I_{RS} is the intensity in steady state (at $t \to \propto$), directly depends on the light-induced refractive-index change in saturation state (Δn^s), as follows [6]:

$$\Delta = \Delta I_R / I_R = A\Delta n^s / (1 + A\Delta n^s) \,, \tag{1}$$

where A is a coefficient related to the conditions of Raman measurements [6]. The value of A is here a constant since all the experimental conditions are identical.

Therefore, from the Raman spectroscopy measurements in the waveguides, we do actually characterize two main photorefractive parameters: the magnitude of the saturated-index change (Δn^s) and the kinetics of the photorefractive response, i.e. the time constant τ. The Δn^s values induced in the various samples are determined by comparing the measured Δ values to known detailed data previously obtained. As seen in Table 1, Δn^s greatly depends on the exchange conditions, but it is worth noting that our elaboration process enables us to increase significantly, to more than thirty times, the photorefractive response of the crystal.

The dependence of Δn^s with the copper concentration in the waveguides is illustrated in Fig. 4 for two levels of residual hydrogen concentration (x), according to the exchange conditions. The differential optical density δD_{Cu} is the optical absorption density measured at $\lambda = 441.6$ nm (the laser wavelength) in the UV–visible absorption spectra of the samples, by using a non-exchange waveguide as reference, and is therefore proportional to the copper concentration. As can be seen, the variation of Δn^s is not strictly monotonous with the copper concentration, Δn^s reaches a maximum for intermediate values of δD_{Cu}. Moreover, there is a crucial influence of the hydrogen concentration x on the Δn^s magnitude. The general behavior with the copper concentration is similar whatever the x value, but for a given Cu content, Δn^s is dramatically reduced for the highest proton concentration. This must be attributed to the degradation of the electro-optical coefficient r_{33} when x increases [7]. It has been shown indeed that $r_{33} \approx (x_t - x)$, where x_t is a threshold-like value of the hydrogen concentration [9]. This is particularly true for the A_3 sample, for which $\Delta n^s = 4.4$ (see Table 1), and is in agreement with the presence of a β_1 phase in the exhanged layer, as evidenced by the IR-absorption measurements (see Fig. 2b).

The decrease of Δn^s observed for the highest Cu concentration is more surprising. It could be qualitatively explained as follows. It's well proved that the photorefractive index change in $LiNbO_3$ depends on the light intensity [6, 20]. Now in this case, as a result of the optical absorption by the copper ions, the dependence of Δn^s on δD_{Cu} is actually directly connected with the effective value of the light intensity (J) inside the waveguide. After a propagation length l, this intensity is expressed as:

$$J = J_{in} \exp(-\alpha l) \,, \tag{2}$$

where J_{in} is the launched intensity into the waveguide and α is the total absorption coefficient at $\lambda = 441.6$ nm. The latter may be regarded, with a good approximation, as the superposition of two independent contributions, i.e. $\alpha = \alpha_U + \alpha_{Cu}$, where α_U and α_{Cu} are the absorption coefficients related to the undoped He-implanted waveguide and to the copper content, respectively. Therefore, for a given propagation length (all the waveguides have similar dimensions) there is in some way a threshold effect beyond which, as the copper concentration increases, the absorption dominates and quenches more and more the photorefractive effect.

The relative change of the photorefractive sensitivity in our He-implanted waveguides in dependence of the combined proton and copper exchange conditions can also be estimated. The photorefractive sensitivity S is known to be defined by the following relation:

$$S = \Delta n^s / (\tau J) \,, \tag{3}$$

where J is the density of light in the waveguide and τ is the time constant (see above). From our measured values of Δn^s and τ, and the relation (3), for an injected intensity into the waveguides of $J_{in} = 12 \times 10^4\,W/m^2$, as seen in Table 1, maximum values of 3×10^{-12} (m^2J^{-1}) and 10^{-8} (m^2J^{-1}) in the undoped and in the Cu-doped samples are obtained, respectively. Therefore, we clearly demonstrate that the copper doping increases dramatically the photorefractive sensitivity of the He-implanted waveguides, up to a factor of more than 3000.

The S and Δn^s values obtained for a given launched intensity in the waveguides, ($J_{in} = 12 \times 10^4\,W/m^2$) are summarized in Table 1, together with the optical absorption results and the conditions of the combined proton and copper exchange process, for the two sets of He^+ implanted waveguides.

Note that the highest photorefractive sensibility is observed in a sample of the B series (B_1), where the light confinement is very likely better, because, according to the TRIM simulation (see Fig. 1), the thickness of the waveguide must be weaker.

6 Conclusion

We have investigated the photoinduced light scattering in photorefractive $LiNbO_3$ waveguides elaborated by a two-step method based on the combination of light-ion implantation for waveguide forming and ion-exchange process for copper doping. The large photorefractive sensitivity obtained demonstrates the marked advantage of this new method against the simple technique of the combined proton and copper exchange. Further improvements of the photorefractive properties should be possible by varying the fabrication conditions, so as to reverse the order of the steps, to optimize the implantation parameters, or to use proton instead of helium ions. The search for the optimum conditions will be subjected to our further investigations.

References

1. V.E. Wood, P.J. Cressman, R.L. Holman, C.M. Veber: In *Photorefractive Materials and their Applications II*, ed. by P. Gunter, J.-P. Huignard (Springer, Berlin, Heidelberg 1989)
2. R.V. Schmidt, P. Kaminov: Appl. Phys. Lett. **25**, 458 (1974)
3. J.L. Jacquel, C.E. Rice, J.L. Veselka: Ferroelectrics **50**, 165 (1983)
4. G.L. Destefanis, J.P. Gaillard, E. Ligeon, S. Valette, B.W. Farmery, P.D. Townsend, A. Perez: J. Appl. Phys. **50**, 7898 (1979)
5. A.D. Novikov, S.G. Odoulov, V.M. Shandarov, S.M. Shandarov: Sov. Tech. Phys. **33**, 969 (1988)
6. S.M. Kostritskii, O.M. Kolesnikov: J. Opt. Soc. Am. B **11**, 1674 (1994)
7. D. Kip, F. Rickermann, E. Krätzig: Opt. Lett. **20**, 1139 (1995)
8. F. Rickermann, D. Kip, B. Gather, E. Kratzig: Phys. Status Solidi A **150**, 763 (1995)
9. S.M. Kostritskii, D. Kip, E. Krätzig: Appl. Phys. B **65**, 517 (1997)
10. P.G. Suchoski, T.K. Findakly, F.G. Leonberger: Opt. Lett. **13**, 1050 (1988)
11. A. Boudrioua, P. Moretti, J.C. Loulergue: J. Non-Cryst. Solids **187**, 443 (1995)
12. D. Kip, B. Kemper, I. Nee, R. Pankrath, P. Moretti: Appl. Phys. B **65**, 511 (1997)
13. P.D. Townsend: Nucl. Instrum. Methods Phys. Res., Sect. B **46**, 18 (1990)
14. T. Bremer, P. Hertel, D. Kollewe: Nucl. Instrum. Methods Phys. Res., Sect. B **34**, 62 (1988)
15. P. Moretti, P. Thevenard, K. Wirl, P. Hertel: Mater. Res. Soc. Symp. Proc. **244**, 323 (1992)
16. P. Moretti, D. Kip, B. Kemper, J. Hekreide: Proc. ECIO-8, Stockholm, 408 (1997)
17. J.F. Ziegler, J.P. Biersack, U. Littmark: *The Stopping and Ranges of Ions in Solids* (Pergamon Press, New York 1988)
18. E. Glavas, L. Zhang, P.I. Chandler, P.D. Townsend: Nucl. Instrum. Methods Phys. Res., Sect. B **32**, 45 (1988)
19. Y.N. Korkishko, V.A. Fedorov: J. Appl. Opt. **83**, 1010 (1997)
20. F. Jermann, M. Simon, E. Krätzig: J. Opt. Soc. Am. B **12**, 2066 (1995)